

1 **Estimating χ and K_T from fast-reponse thermistors on traditional shipboard**

2 **CTDs: sources of uncertainty and bias.**

3 Andy Pickering*

4 *College of Earth, Ocean, and Atmospheric Sciences, Oregon State University, Corvallis, OR.*

5 Jonathan Nash

6 *College of Earth, Ocean, and Atmospheric Sciences, Oregon State University, Corvallis, OR.*

7 Jim Moum

8 *College of Earth, Ocean, and Atmospheric Sciences, Oregon State University, Corvallis, OR.*

9 Jen MacKinnon

10 *UCSD / Scripps Institute of Oceanography*

11 **Corresponding author address:* College of Earth, Ocean, and Atmospheric Sciences, Oregon State
12 University, Corvallis, OR.

13 E-mail:

ABSTRACT

The acquisition of turbulence data from traditional shipboard CTD casts is attractive as it has the potential to dramatically increase the amount of deep-ocean mixing observations globally. While data from shear-probes are easily contaminated by motion of the instrument platform, the measurement of temperature gradient is relatively insensitive to vehicle vibration, making it possible to measure temperature gradient from a shipboard CTD rosette. The purpose of this note is to investigate the error and bias in estimating the rate of dissipation of temperature variance χ and turbulent diffusivity K_T from traditional CTD casts. The most significant source of error is associated with the fact that fast-response FP07 thermistors resolve only a fraction of the temperature gradient variance at the fallspeed of typical CTD casts. Assumptions must be made about the wavenumber extent of the temperature gradient spectrum, which scales with the rate of dissipation of turbulent kinetic energy, a quantity that is not directly measured. Here we utilize observations from a microstructure profiler to demonstrate the validity of the method of estimating χ from thermistor data, and to assess uncertainty and bias. We then apply this methodology to temperature gradient profiles obtained on CTD (the CTD- χ -pod), and compare these to microstructure profiles obtained almost synoptically, at both the equator and in Luzon Strait. CTD- χ -pod estimates of χ compare favorably to the direct microstructure measurements and demonstrate that the χ -pod method is not significantly biased. This supports the utility of the measurement as part of the global repeat hydrography program cruises, during which this type of data has been acquired during the past few years.

38 1. Introduction

39 Turbulent mixing affects the distribution of heat, salt, and nutrients throughout the global ocean.
40 Diapycnal mixing of cold, dense water with warmer water above maintains the abyssal overturning
41 circulation Munk (1966); Munk and Wunsch (1998), which affects global climate. Due to sparse
42 observations and the small scales at which mixing occurs, it is usually parameterized in climate
43 models. Recent investigations have demonstrated that these models are sensitive to the magnitude
44 and distribution of mixing Melet et al. (2013). Better measurements are needed to constrain mixing
45 and develop more accurate parameterizations.

46 Direct measurement of mixing with microstructure profilers equipped with shear probes is ex-
47 pensive, time-intensive, and requires considerable care and expertise. Moreover, tethered profilers
48 can't reach abyssal depths, requiring autonomous instruments to get deeper than ~ 1000 -2000 m.
49 As a result, existing measurements of diapycnal mixing, especially in the deep ocean, are sparse
50 Waterhouse et al. (2014). In order to obtain estimates over a larger area, considerable work has
51 gone into inferring mixing from larger scales where measurements are easier to obtain. One pop-
52 ular method is the use of Thorpe scales, where diapycnal mixing is inferred from inversions in
53 profiles of temperature or density Thorpe (1977); also cite Dillon(1982)?. There are some ques-
54 tions about the validity of the assumptions made, though several studies indicate relatively good
55 agreement with microstructure and other observations. However, the size of resolvable overturn
56 is limited by the profiling speed and instrument noise (Galbraith and Kelley 1996). Parameter-
57 izations based on profiles of shear and/or strain have also been developed to estimate diapycnal
58 mixing (this actually started with the Gregg-Henyey form) Kunze et al. (2006); Polzin et al. (2013);
59 Whalen et al. (2012, 2015). However, they rely on a series of assumptions about the cascade of
60 energy from large to small scales that are often violated; numerous studies (i.e., Waterman et al)

61 have shown that there is significant uncertainty associated with this method; in that there can be a
62 consistent bias in a particular region, yet the sense of the bias (i.e., overpredict vs. underpredict) is
63 not aprior known.

64 Measurement of turbulence from velocity shear variance (to compute the dissipation rate of
65 turbulent kinetic energy ϵ) is challenging on moorings or profiling platforms because there is
66 usually too much vibration/package motion for shear-probes to be useful. Other methods (i.e.,
67 optics or acoustics) may hold some promise, but lack of scatterers often precludes this type of
68 measurement, especially in the abyss. In addition, shear probes only provide ϵ , not the mixing of
69 scalars, K , which is often inferred from ϵ by assuming a mixing efficiency; Osborne 80). A more
70 direct measure of the turbulent mixing is obtained from the dissipation rate of temperature variance
71 χ Osborn and Cox (1972). This has the advantage that temperature and temperature gradient can
72 be computed However, the spectrum of temperature gradient extends to very small scales, so that
73 its spectrum is seldom fully resolved (and unlike shear variance, the wavenumber extent of the
74 spectrum is not related to the amplitude of the temperature (or temperature gradient) spectrum).
75 Assumptions about the spectral shape (Kraichnan vs. Batchelor, and the value of the “constant” q)
76 and its wavenumber extent (governed by the Batchelor wavenumber $k_b = \dots$; Batchelor 1959) are
77 thus necessary to determine χ unless measurements capture the full viscous-diffusive subrange of
78 turbulence (i.e., down to scales $\Delta x \sim 1/k_b \sim 1\text{mm}$), a criterion seldom achieved. To resolve this,
79 we follow the assumptions of Alford (appendix) and Moum and Nash... and make the assumption
80 that $K_T = K_\rho$ to determine the dissipation rate as $\epsilon_\chi = (N^2 \chi) / (2\Gamma \langle dT/dz \rangle^2)$, permitting the
81 k_b to be estimated.

82 Then some leftover text:

83 This method has the advantage that χ is not very sensitive to platform accelerations. χ -pods are
84 self-contained, internally recording instruments that were designed to measure mixing using this
85 method on moorings and profiling instruments Moum and Nash (2009).

86 The goal of this paper is to outline and validate the methods used to compute χ and K_T with
87 χ -pods mounted on CTDs. We do this by applying our processing methods to profiles of turbulent
88 temperature fluctuations measured by the ‘Chameleon’ microstructure profiler, which provides a
89 direct test of our methodology. Because Chameleon is a loosely tethered profiler equipped with
90 shear probes (Moum et al 1995), it directly measures ε and allows us to test our assumptions.
91 Specifically, it allows us to determine biases associated with computing χ from partially-resolved
92 temperature alone, as compared to that when it is computed by including knowledge of the dis-
93 sipation rate, which constrains the wavenumber extent of the scalar spectra. After establishing
94 that the method works, we then compare CTD-chipod profiles to nearby microstructure profiles
95 made during two experiments. Finally, preliminary sections of χ and K_T from χ -pods deployed
96 on several GO-SHIP cruises are presented.

97 **2. Data and Methods**

98 I would start with 1-2 paragraphs that expand some of the details of the method, like explaining
99 why the spectrum is not fully resolved, at what dissipation rates, profiling speeds it is not resolved,
100 and then this provides some justification for our methods and why methods that assume that the
101 peak of the temperature spectrum is measured, simply can’t work. Once you make that assumption
102 / assertion, then I think the method we propose is one of the few that can work. But then I think
103 you still want to test those other methods.

104 *a. EQ08*

105 Data were collected during the EQ08 experiment on the R/V ? in 2008. A total of xx Chameleon
106 profiles were made. Most Chameleon profiles were made to depth of about 250m, with CTD
107 casts going deeper. Profiles were located within xxkm of moorings equipped with moored χ pods.
108 Perlin and Moum (2012) used these data to compare with Chameleon profiles and found general
109 agreement.

110 *b. EQ14*

111 Data were collected on the R/V Oceanus in Fall 2014 during the EQ14 experiment to study
112 equatorial mixing. More than 2700 Chameleon profiles were made, along with 35 CTD-chipod
113 profiles bracketed by chameleon profiles in order to maintain calibrations during the cruise. Most
114 Chameleon profiles were made to depth of about 250m, with CTD casts going to 500m or deeper.
115 Most CTD casts were bracketed by Chameleon profiles. *is there a paper by Jim or Sally to
116 reference here?*

117 *picture of CTD-chipod setup?*

118 *c. CTD-chipod Data Processing*

119 ***I think you might want to start this section with some of the details that are currently in
120 section 2e, which is the ultimate equation that needs to be solved. Then I think it follows more
121 logically to explain the limitations with the measurement, and why we need to do all the other
122 parts that are outlined below.

123 Also, you might want to include a figure showing something about removing depth loops (like
124 the figure in the proposal), and then also quantify how much data needs to be thrown out as a
125 function of sea-state. All of this was in the proposal.

The basic outline for processing each CTD- χ -pod profile is as follows:

1. The correct time-offset for the χ -pod clock is determined by aligning dp/dt from the 24Hz CTD data to vertical velocity calculated by integrating vertical accelerations measured by the χ -pod. χ -pod clock drift is small, typically on the order of 1 sec/week.
2. The conversion from voltage to SI temperature (ITS-90) is performed using a polynomial fit of chipod thermistors to CTD temperature.
3. Depth loops are identified and flagged in the 24Hz CTD data. χ -pod data during these times are discarded since the sensor is not seeing ‘clean’ fluid. Even for profiles that are significantly affected by ship heaving, good segments of data are obtained over a majority of the water column.
4. Buoyancy frequency N^2 and temperature gradient dT/dz are computed from 1m binned CTD data. Resorted or not? Is this really the case?
5. Half-overlapping 1 sec windows of data are used to estimate χ , ϵ , and K_T following the methods described in Moum and Nash (2009), which are repeated below for reference. In this case, the flow speed past the sensor is assumed to be equal to the fall speed of the package.

d. Thermistor Response Correction

start with something like... sensors only respond to approx 10-20 Hz, so corrections need to be applied to the spectra if data if the variance at higher wavenumbers than this is to be used in the computations...

Before performing the χ pod calculations, the temperature gradient spectra are corrected to account for the response of the thermistor. Previous studies of thermistor response corrections have

147 found a variety of results (Gregg, Lueck, etc.). We choose a filter of the form

$$H^2(f) = \frac{1}{[1 + (f/f_c)^2]} \quad (1)$$

148 with cutoff frequency $f_c = 10\text{Hz}$ to apply to the temperature gradient frequency spectra to cor-
 149 rect for lost variance. Applying this response correction improves the agreement between with
 150 chameleon χ (as seen in later section), especially at higher magnitudes. The response is expected
 151 to vary with individual thermistor, but measuring the response of every thermistor is not practical
 152 so we use this generic response. An example spectrum is shown in Figure 3. Note that we only in-
 153 tegrate up to a wavenumber of $15/u$, where the observed spectrum rolls off and u is the flowspeed
 154 past the sensor. χ estimated from the corrected spectrum agrees better with the true chameleon
 155 value.

156 Question - do you want to determine the f_c for every sensor by finding a section of very high
 157 epsilon, and then simply assuming a $k^{1/3}$ shape and minimizing error over some wavenumber
 158 band? That would be one objective method. I think you could automate this (and it could even
 159 include the wake (or would could even use the wave sections explicitly for this purpose!!!)

160 *e. Iterative Method for estimating χ*

161 For each 1 second window, χ is estimated via the following procedure (Moum and Nash 2009).

162 For isotropic turbulence,

$$\chi_T = 6D_T \int_0^\infty \Psi_{T_x}(k) dk \quad (2)$$

163 where D_T is the thermal diffusivity and $\Psi_{T_x}(k)$ is the wavenumber spectrum of dT/dx .

164 Note that dT/dx is not measured; dT/dt is measured, and dT/dx is inferred from Taylor's
 165 frozen flow hypothesis

$$\frac{dT}{dx} = \frac{1}{u} \frac{dT}{dt} \quad (3)$$

The wavenumber extent of the spectrum depends on the Batchelor wavenumber k_b , which is related to ε :

$$k_b = [\varepsilon / (\nu D_T^2)]^{1/4} \quad (4)$$

Assume that $K\rho = K_T$ and $K\rho = \Gamma\varepsilon/N^2$. Then dissipation rate is computed as

$$\varepsilon_\chi = \frac{N^2 \chi_T}{2\Gamma < dT/dz >^2} \quad (5)$$

The thermistors do not measure spectrum to k_b typically. So the measured portion of the spectrum must be fit to a theoretical spectrum. Use Kraichnan form of theoretical scalar spectrum.

The variance between the measured $[\Phi_{T_x}(k)]_{obs}$ and theoretical $[\Phi_{T_x}(k)]_{theory}$ spectra at resolved wavenumbers is assumed to be equal:

$$\begin{aligned} & \int_{k_{min}}^{k_{max}} [\Phi_{T_x}(k)]_{obs} dk \\ &= \int_{k_{min}}^{k_{max}} [\Phi_{T_x}(k)]_{theory} dk \quad (6) \end{aligned}$$

An iterative procedure is used to fit and calculate ε :

1. First we estimate χ_T based on an initial guess of k_b . We set $k_{max} = k_b/2$ or to a wavenumber equivalent to $f = 40$ Hz [i.e., $k_{max} = 2\pi(40)/u$], whichever is smaller.
2. We then use Eq. (5) to refine our estimate of k_b and recompute χ_T using Eqs. (2) and (6).
3. This sequence is repeated and converges after two or three iterations.

Note that this procedure is equivalent to the explicit formulation of Alford thesis, except we use the Kraichnan spectrum.

180 *f. flowspeed past the sensor*

181 Want to explain how you do this? With or without ADCP data? And consequences of omitting

182 $u_{horizontal}$

183 **3. Oceanographic Setting and Conditions**

184 Brief overview of dynamics in study region? Do Jim or Sally have a paper on EQ14 we could
185 cite?

186 **4. Example Spectra**

187 * Show some example spectra w/ fitted Kraichnan spectra. Show for different ranges of χ /
188 ϵ ? Note at higher ϵ , less of spectra is resolved etc., . ?*

189 Figure 4 shows the fraction of k_b resolved for all 1-sec data windows in EQ14. The majority
190 of spectra resolve less than 30% of the Batchelor wavenumber (computed using chameleon ϵ).
191 The maximum observed wavenumber depends on the maximum frequency resolved (15Hz here)
192 and the fallspeed of the instrument (typically near 1m/s for chameleon, as well as CTD- χ pods).
193 Because only a small part of the spectrum is resolved, spectra curve-fitting methods (ie Ruddick
194 2000) do not work as well; instead we use the iterative χ pod method.

195 That last statement could be used up-front to justify our methods.

196 **5. Results - Direct Test of χ – pod Method**

197 ***use present tense most of the time???

198 We first perform a test of our method of estimating χ by applying the χ pod method to each
199 Chameleon profile, using only the FP07 thermistor data, following equation XX. These results,
200 which we will refer to as χ_χ , are compared with χ_ϵ , computed using equation YY, in which k_b

is computed directly from shear-probe derived ε instead of the iterative method (eq ZZ). Qualitatively, χ_χ and χ_ε show very similar depth and time patterns (Figure 5), suggesting the method generally works. A more quantitative comparison is made with a 2-D histogram (Figure 7,8), which shows that the two are well-correlated. There is a slight tendency for χ_χ to underestimate χ_ε at larger values of χ_ε in the EQ14 data. This relationship is sensitive to the parameter ‘fmax’, which sets the maximum frequency the temperature gradient spectrum is integrated up to. This sensitivity is examined in more detail in the appendix. We conclude that estimates of χ from the χ_{pod} method are accurate.

6. Results - CTD χ – *pod* - Chameleon Comparison

Having shown that the method works, we now compare χ from CTD-mounted χ_{pods} to χ_ε . In these we expect a stronger coupling to the ship heaving, more vibration, and artificial turbulence created by the rosette. We first compare CTD- χ_{pod} profiles to the mean of chameleon profiles bracketing each cast, both averaged in 5m depth bins (Figure 9). The two appear to be correlated, with considerable scatter. However, we expect significant natural variability even between chameleon profiles. Scatter plots of before/after chameleon profiles (not shown), typically separated by about an hour, show a similar level of scatter, suggesting that the observed differences (Figure 9) can be explained by natural variability in turbulence. Average profiles from all CTD-chameleon pairs (Figure 11) overlap within 95% confidence limits at all depths where there exists good data for both. Averages of subsets of profiles clustered in position/time (not shown) also agree.

7. Results - IWISE CTD χ – *pod*-VMP Comparisons

** Keep or get rid of this section? Don’t have chi from Harper’s VMP, could try to get it...**

8. Discussion

* Talk about other possible issues* * talk about plan going forward for deployments etc* * show one or 2 sections from P16N or other cruise?*

We have shown that χ can be accurately estimated from χ pods attached to CTD rosettes. The method also estimates ε , but we have not discussed it here since it involves more assumptions and uncertainties. One major assumption is the mixing efficiency Γ . A value of 0.2 is commonly assumed, but evidence suggests this may vary significantly. The χ pod method also assumes that $K_T = K_\rho$. Even if ε estimates have a large uncertainty, χ and K_T are robust and should be useful to the community.

The goal of CTD- χ pods is to expand the number and spatial coverage of ocean mixing observations. We have already deployed instruments during several experiments (IWISE, TTIDE) and on several GO-SHIP repeat-hydrography cruises. We plan to continue regular deployment on GO-SHIP and similar cruises, adding χ and K_T to the suite of variables measured and enabling scientists to explore relationships between these and other variables. The expanding database of mixing measurements from CTD- χ pods will also enable testing of other commonly-used or new mixing parameterizations.

9. Conclusions

- The χ pod method was directly applied to temperature gradients measured by the chameleon microstructure profiler on more than 4000? profiles during the EQ08 and EQ14 cruises. The estimated χ agrees well with χ calculated using ε from shear probes over a wide range of magnitudes (Figure 7).

- CTD- χ pods were also compared to nearby chameleon profiles during the cruise. Averaged profiles of χ agree within 95% confidence limits.
- We conclude that estimates of χ and K_T from the CTD- χ pod platform are robust and reliable.

Acknowledgments. Harper Simmons provided microstructure data. Data were collected during IWISE, which was funded by ONR. Others...

APPENDIX A

Sensitivity to ‘fmax’

Here we investigate the sensitivity of the χ pod calculations to the parameter ‘fmax’, the upper limit for integrating the temperature gradient spectrum. In practice, fmax is limited by the frequency at which the FP07 thermistor rolls off. This varies slightly between individual thermistors, but is typically between 10-15 Hz for the sensors we use (show example spectra?). Figure ? shows χ_χ vs χ_ϵ for different values of fmax.

APPENDIX B

Sensitivity to flowspeed

Here we investigate the sensitivity of the χ pod calculations to flowspeed, which is used to convert temperature gradient spectra from the frequency domain to the wavenumber domain via Taylor’s frozen flow hypothesis. In this data, we have assumed the flow speed is equal to the vertical speed of the CTD rosette, determined from the recorded pressure. In most locations, this is likely a good approximation. However, when horizontal velocities are large, the true flowspeed past the sensor will differ. To test the sensitivity of the χ pod method to flowspeed, we repeated the calculations with a constant offset added to the flowspeed. The results show...

See Figure 13.

B1. Sensitivity to N^2 and dT/dz

We investigated the sensitivity of the calculations to N^2 , dT/dz . The iterative method to estimate chi requires the background stratification N^2 and temperature gradient dT/dz . We investigated the sensitivity of the results to the choice of scale over which these are computed or smoothed.

The estimate of χ is only weakly dependent on these scales, while dissipation rate and diffusivity are more strongly affected because they are linearly related to these values.

APPENDIX C

Test of MLE fitting method

Test spectra fitting method of Ruddick et al 2000? Doesn't work well since we don't resolve that much of spectrum?

References

Kunze, E., E. Firing, J. Hummon, T. K. Chereskin, and A. Thurnherr, 2006: Global abyssal mixing inferred from lowered ADCP shear and CTD strain profiles. *Journal of Physical Oceanography*, **36** (8), 1553–1576.

Melet, A., R. Hallberg, S. Legg, and K. L. Polzin, 2013: Sensitivity of the ocean state to the vertical distribution of internal-tide-driven mixing. *J. Phys. Oceanogr.*, **43** (3), 602–615, doi: <http://dx.doi.org/10.1175/JPO-D-12-055.1>.

Moum, J., and J. Nash, 2009: Mixing measurements on an equatorial ocean mooring. *J. Atmos. Ocean. Tech.*, **26**, 317–336.

285 Munk, W., and C. Wunsch, 1998: Abyssal recipes II: energetics of tidal and wind mixing. *Deep-*
286 *Sea Res. Part I*, **45**, 1977–2010.

287 Munk, W. H., 1966: Abyssal recipes. *Deep-Sea Res.*, **13**, 707–730.

288 Osborn, T. R., and C. S. Cox, 1972: Oceanic fine structure. *Geophys. Fluid Dyn.*, **3**, 321–345.

289 Perlin, A., and J. Moum, 2012: Comparison of thermal variance dissipation rates from moored and
290 profiling instruments at the equator. *Journal of Atmospheric and Oceanic Technology*, **29** (9),
291 1347–1362.

292 Polzin, K. L., A. C. Naveira Garabato, T. N. Huussen, B. M. Sloyan, and S. N. Waterman, 2013:
293 Finescale parameterizations of turbulent dissipation. *Rev. Geophys.*, **submitted**.

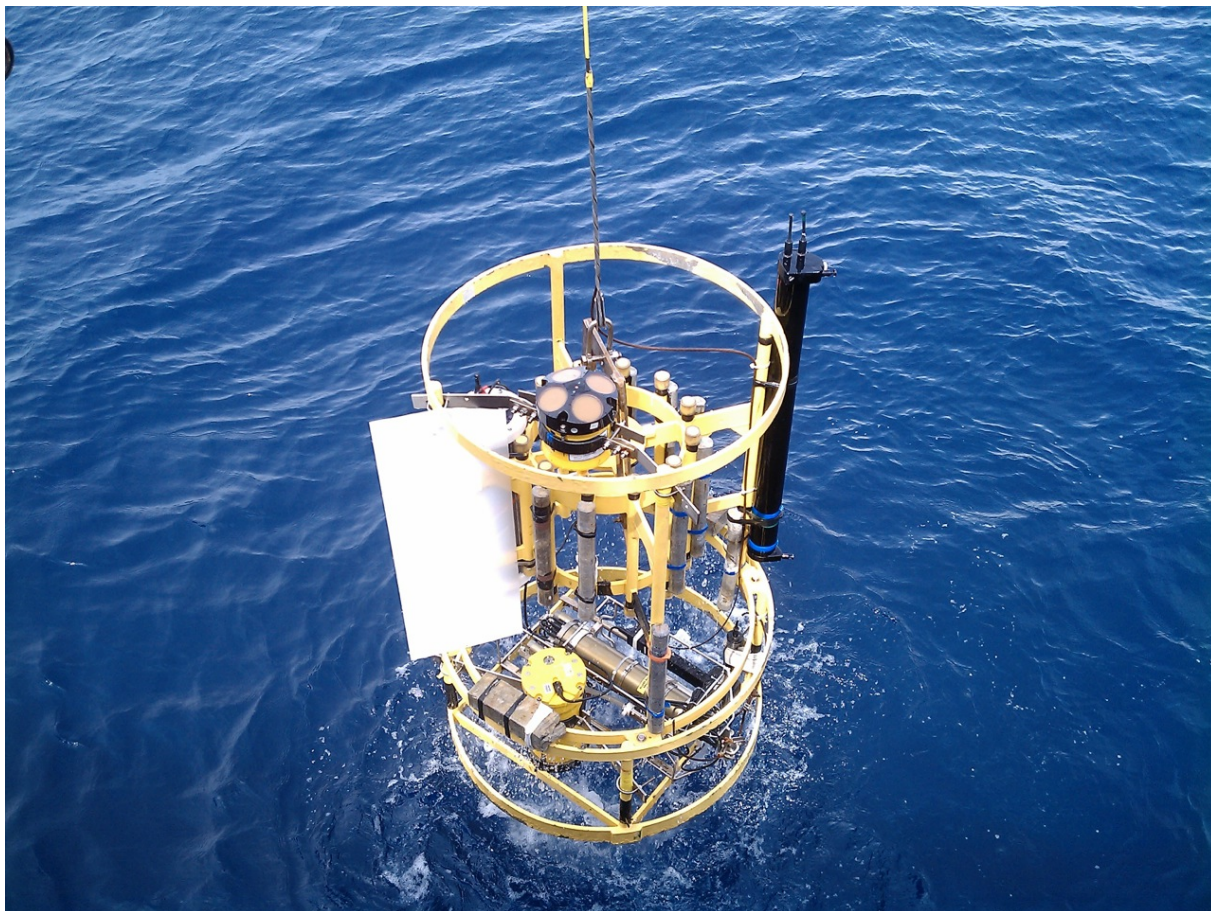
294 Thorpe, S., 1977: Turbulence and mixing in a Scottish Loch. *Philos. Trans. R. Soc. London Ser.*
295 *A*, **286**, 125–181.

296 Waterhouse, A. F., and Coauthors, 2014: Global patterns of diapycnal mixing from measurements
297 of the turbulent dissipation rate. *J. Phys. Oceanogr.*, **44** (7), 1854–1872.

298 Whalen, C. B., J. A. MacKinnon, L. D. Talley, and A. F. Waterhouse, 2015: Estimating the
299 mean diapycnal mixing using a finescale strain parameterization. *Journal of Physical Oceanog-*
300 *raphy*, **45** (4), 1174–1188, doi:10.1175/JPO-D-14-0167.1, URL [http://dx.doi.org/10.1175/](http://dx.doi.org/10.1175/JPO-D-14-0167.1)
301 [JPO-D-14-0167.1](http://dx.doi.org/10.1175/JPO-D-14-0167.1).

302 Whalen, C. B., L. D. Talley, and J. A. MacKinnon, 2012: Spatial and temporal variabil-
303 ity of global ocean mixing inferred from argo profiles. *Geophys. Res. Lett.*, **39** (L18612),
304 doi:10.1029/2012GL053196.

| | | |
|-----|--|----|
| 305 | LIST OF FIGURES | |
| 306 | Fig. 1. Photo of <i>R/V Revelle</i> CTD rosette with χ -pod attached (black unit at upper right). *To be | |
| 307 | replaced by photo from EQ14* | 18 |
| 308 | Fig. 2. Example timeseries from one CTD cast. a) CTD pressure. b) Fallspeed of CTD (dp/dz) | |
| 309 | .c) Accelerations measured by χ -pod. d) Temperature from CTD and χ -pod (calibrated). | |
| 310 | e) Temperature derivative dT/dt measured by χ -pod sensor 1. f) Temperature derivative | |
| 311 | dT/dt measured by χ -pod sensor 2. | 19 |
| 312 | Fig. 3. Example temperature gradient spectra from EQ14. Solid blue and black lines show the | |
| 313 | observed spectra, before and after a response correction was applied. Dashed lines show the | |
| 314 | theoretical Kraichnan spectra for the χ pod estimates. Purple line is Kraichnan spectra for | |
| 315 | chameleon χ and ϵ . Vertical dashed line indicates the maximum wavenumber used in the | |
| 316 | χ pod calculation. | 20 |
| 317 | Fig. 4. Histogram of the ratio of the maximum observed wavenumber k_{max} to the Batchelor | |
| 318 | wavenumber k_b for all profiles in EQ14. | 21 |
| 319 | Fig. 5. Depth-time plots of χ from both methods for EQ14 data. | 22 |
| 320 | Fig. 6. Depth-time plots of χ from both methods for EQ08 data. | 23 |
| 321 | Fig. 7. 2D histogram of χ from chameleon (x-axis) and chipod method (y-axes). Each panel uses a | |
| 322 | different value of fmax. | 24 |
| 323 | Fig. 8. EQ08: 2D histogram of χ from chameleon (x-axis) and chipod method (y-axes). Each panel | |
| 324 | uses a different value of fmax. | 25 |
| 325 | Fig. 9. Scatter plot of χ from CTD- χ pod profiles versus the mean of bracketing chameleon profiles. | |
| 326 | Black dashed line shows 1:1, red are ± 10 X. **replace with histogram of ratios, or combine | |
| 327 | into one figure?*** | 26 |
| 328 | Fig. 10. Histogram of \log_{10} of the ratio of χ for nearby casts. One line is for CTD- χ pod profiles | |
| 329 | versus the bracketing chameleon profiles. Another line is for the before vs. after chameleon | |
| 330 | profiles. *Note bias is small/zero, and the variability (spread) between CTD/cham is similar | |
| 331 | to the natural variability between cham profiles.* | 27 |
| 332 | Fig. 11. Time mean of χ for all CTD- χ pod - chameleon cast pairs, with 95% bootstrap confidence | |
| 333 | intervals. | 28 |
| 334 | Fig. 12. Example chipod data from P16N. *need to clean up* | 29 |
| 335 | Fig. 13. Histogram of % error for χ computed with constant \pm fspd added. | 30 |



336 FIG. 1. Photo of *R/V Revelle* CTD rosette with χ -pod attached (black unit at upper right). *To be replaced by
337 photo from EQ14*

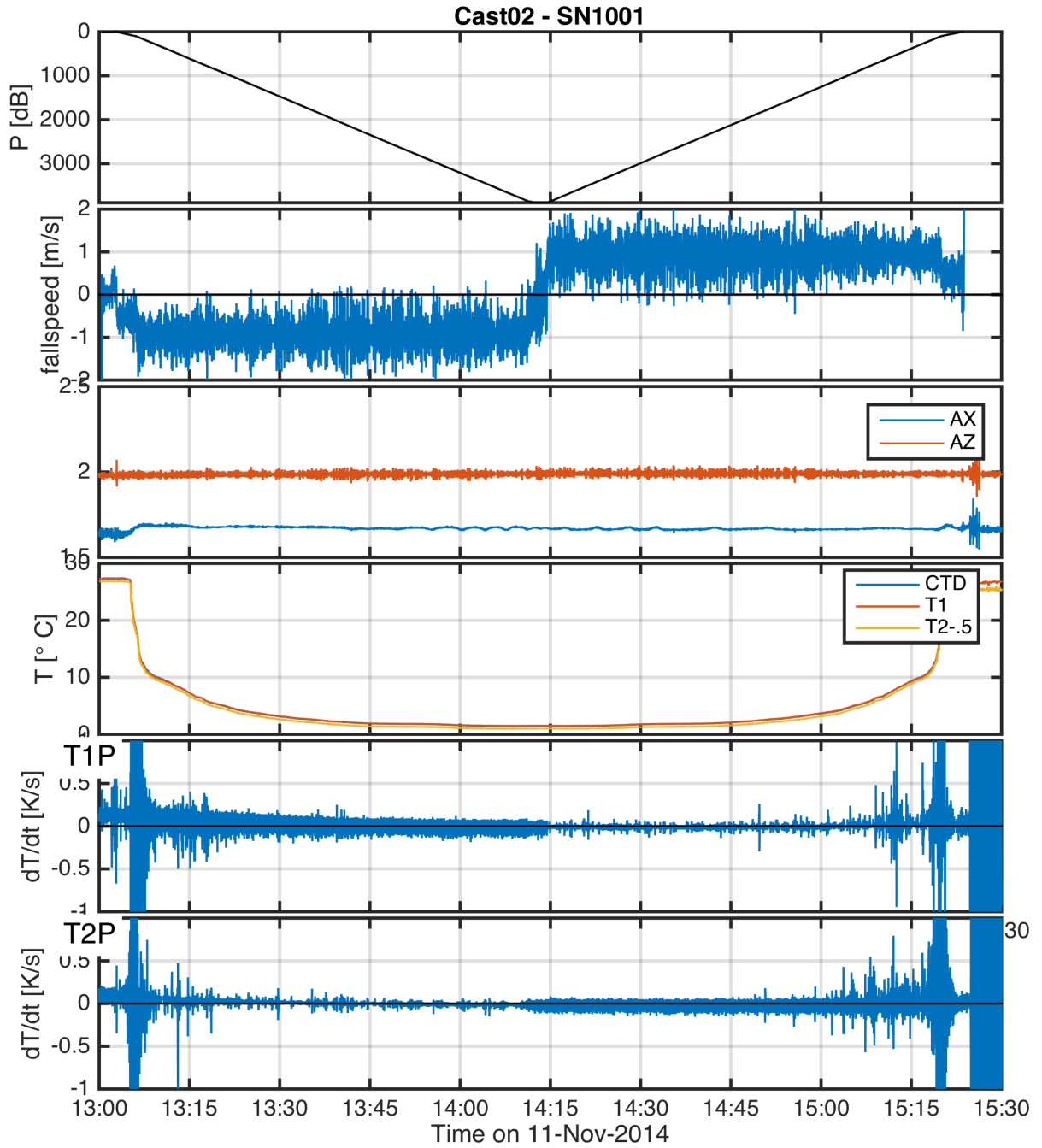


FIG. 2. Example timeseries from one CTD cast. a) CTD pressure. b) Fallspeed of CTD (dp/dz). c) Accelerations measured by χ -pod. d) Temperature from CTD and χ -pod (calibrated). e) Temperature derivative dT/dt measured by χ -pod sensor 1. f) Temperature derivative dT/dt measured by χ -pod sensor 2.

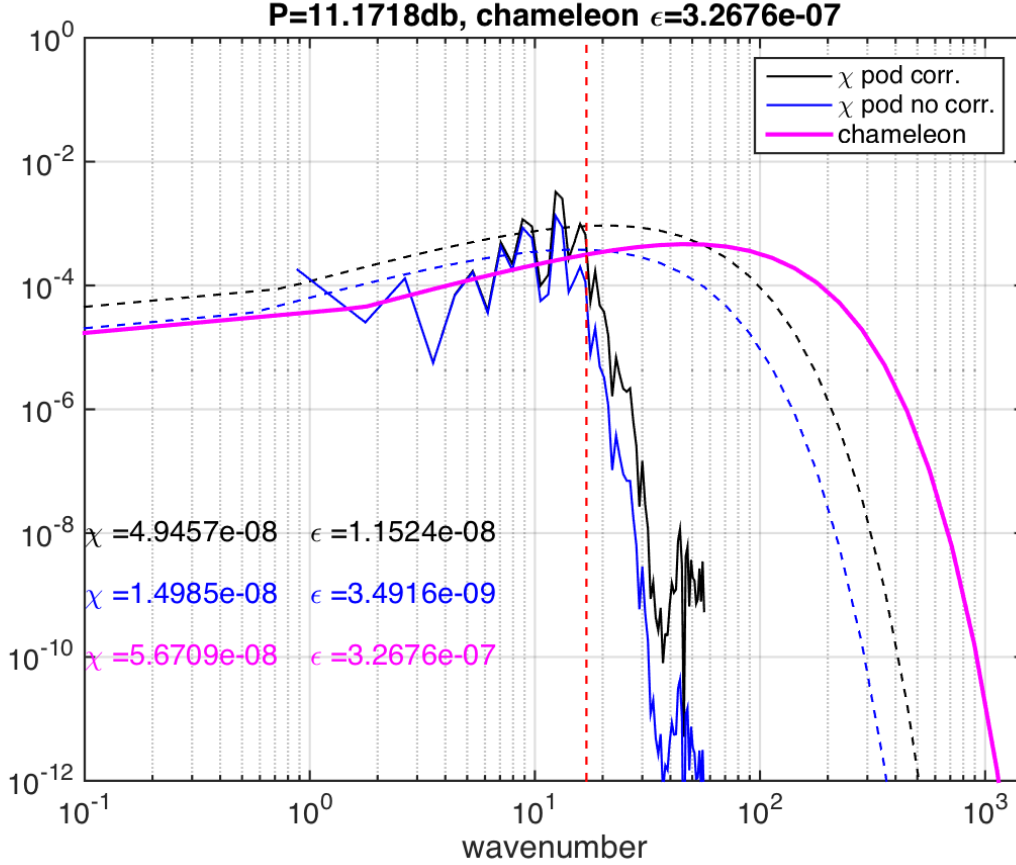


FIG. 3. Example temperature gradient spectra from EQ14. Solid blue and black lines show the observed spectra, before and after a response correction was applied. Dashed lines show the theoretical Kraichnan spectra for the χ pod estimates. Purple line is Kraichnan spectra for chameleon χ and ϵ . Vertical dashed line indicates the maximum wavenumber used in the χ pod calculation.

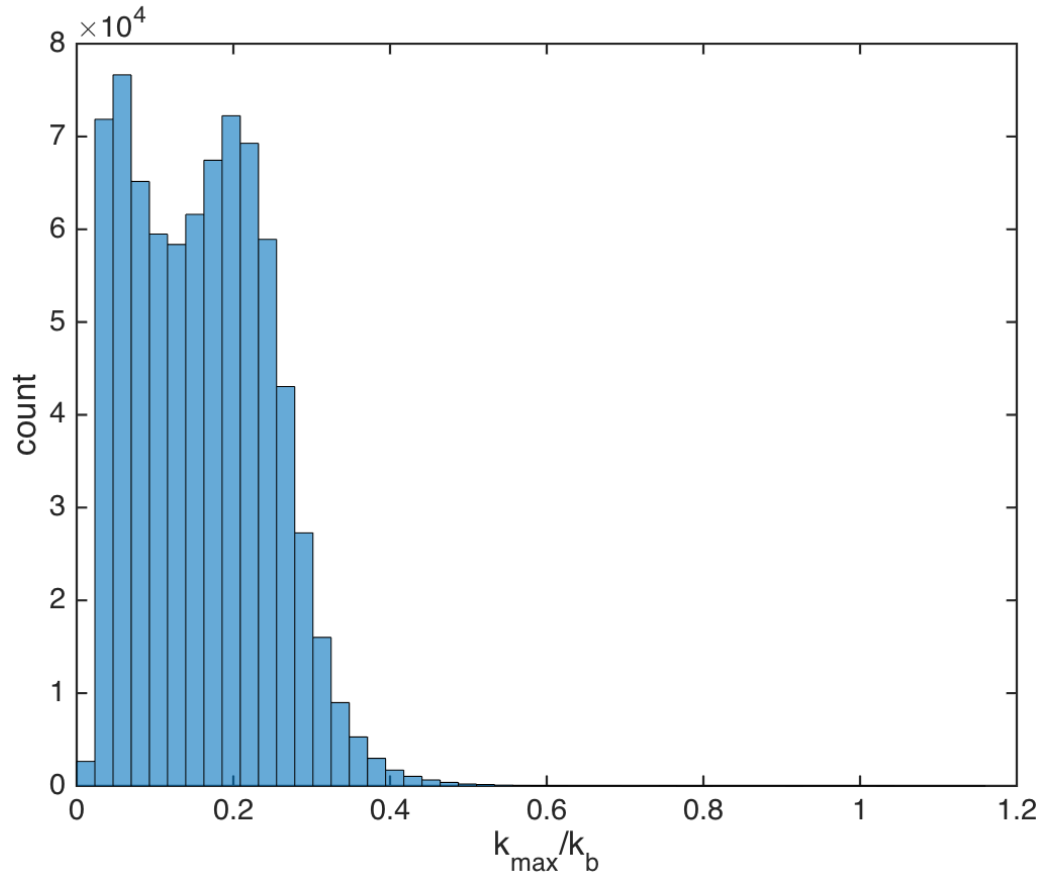


FIG. 4. Histogram of the ratio of the maximum observed wavenumber k_{\max} to the Batchelor wavenumber k_b for all profiles in EQ14.

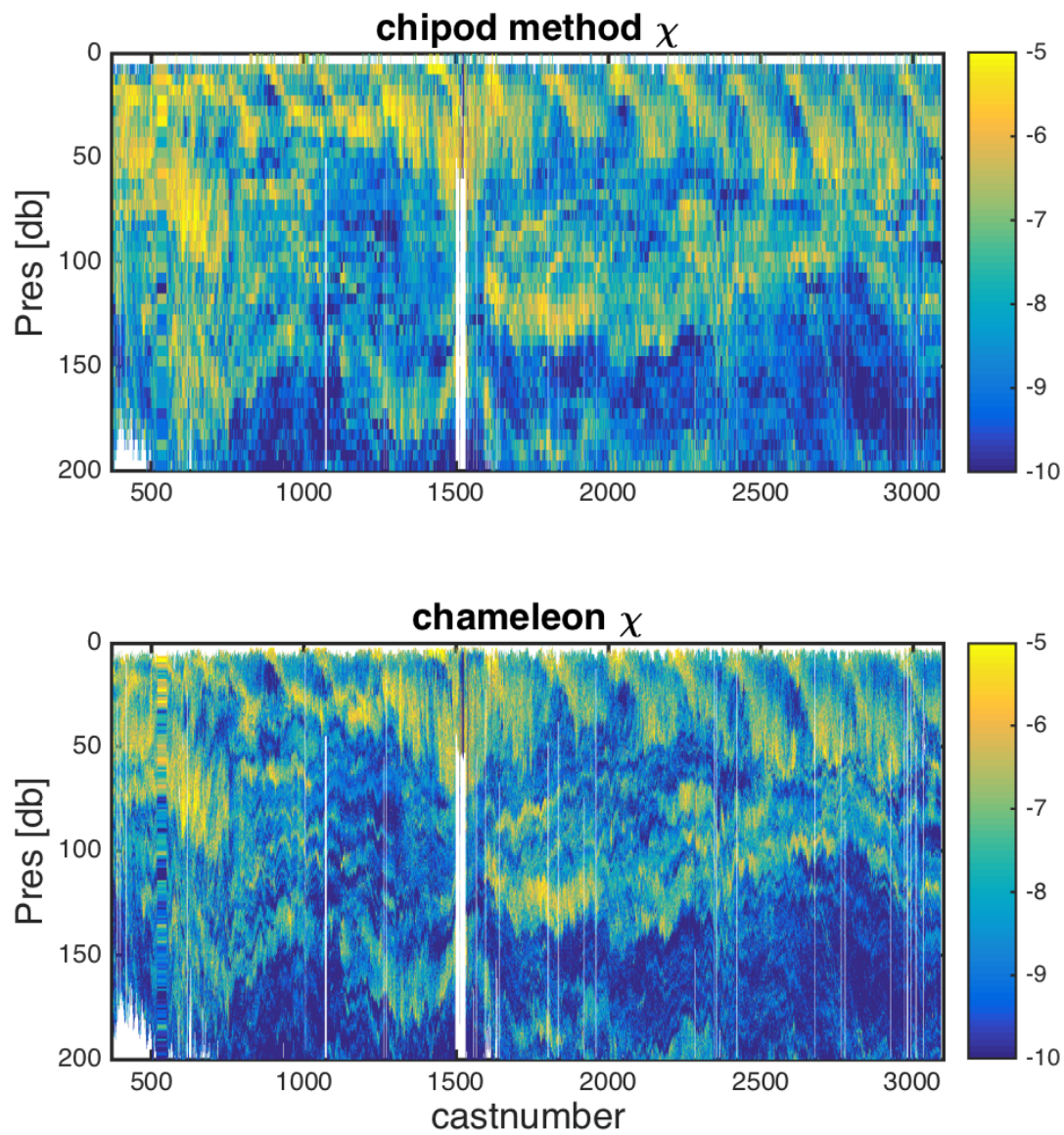


FIG. 5. Depth-time plots of χ from both methods for EQ14 data.

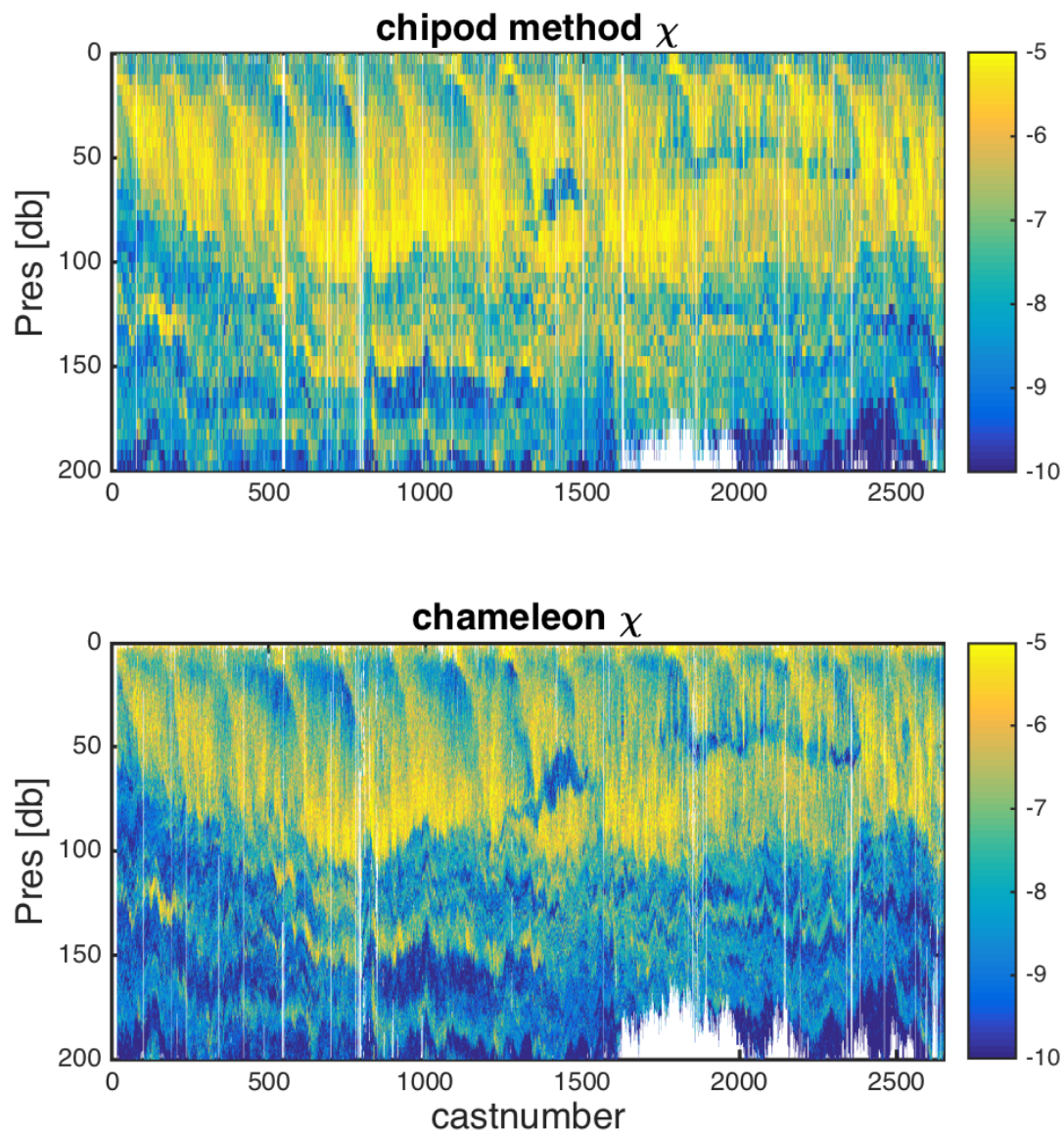


FIG. 6. Depth-time plots of χ from both methods for EQ08 data.

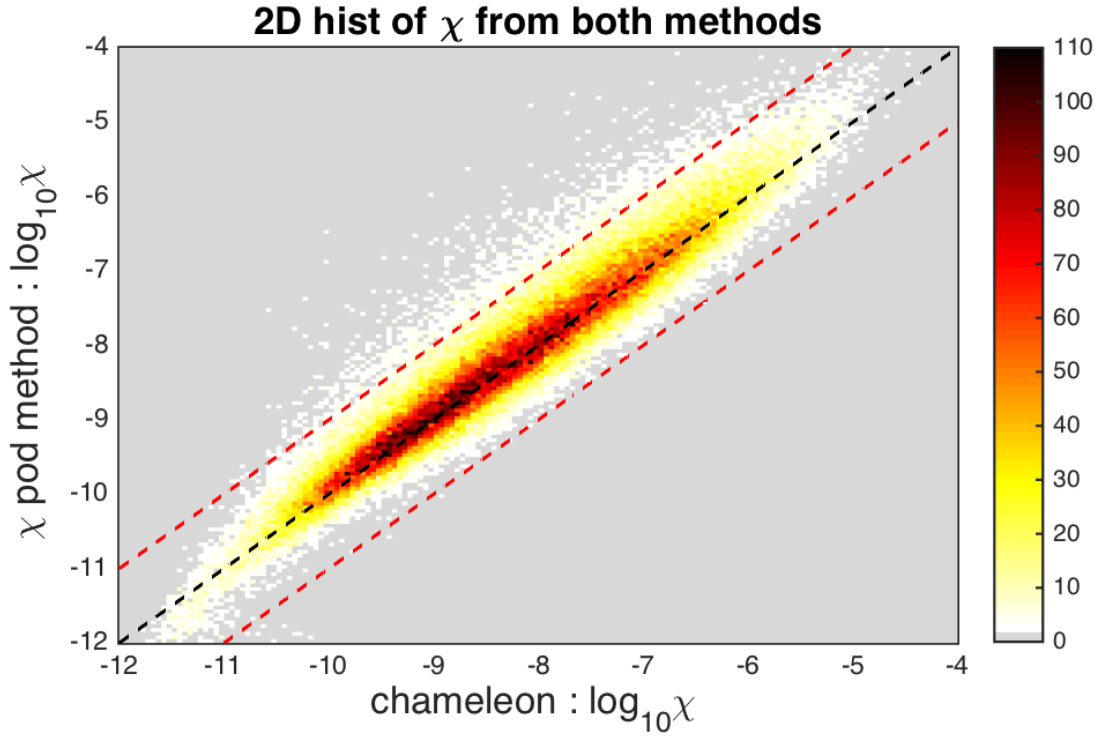


FIG. 7. 2D histogram of χ from chameleon (x-axis) and chipod method (y-axes). Each panel uses a different value of fmax.

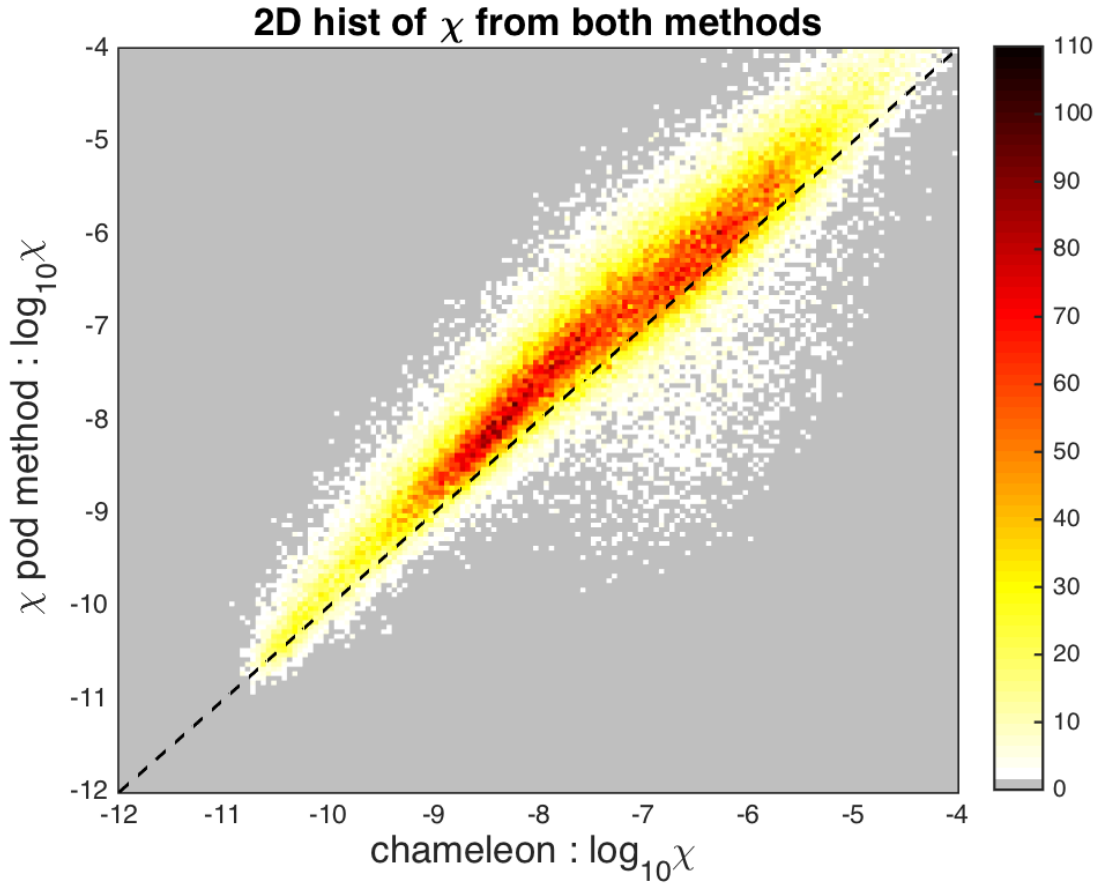


FIG. 8. EQ08: 2D histogram of χ from chameleon (x-axis) and chipod method (y-axes). Each panel uses a
different value of fmax.

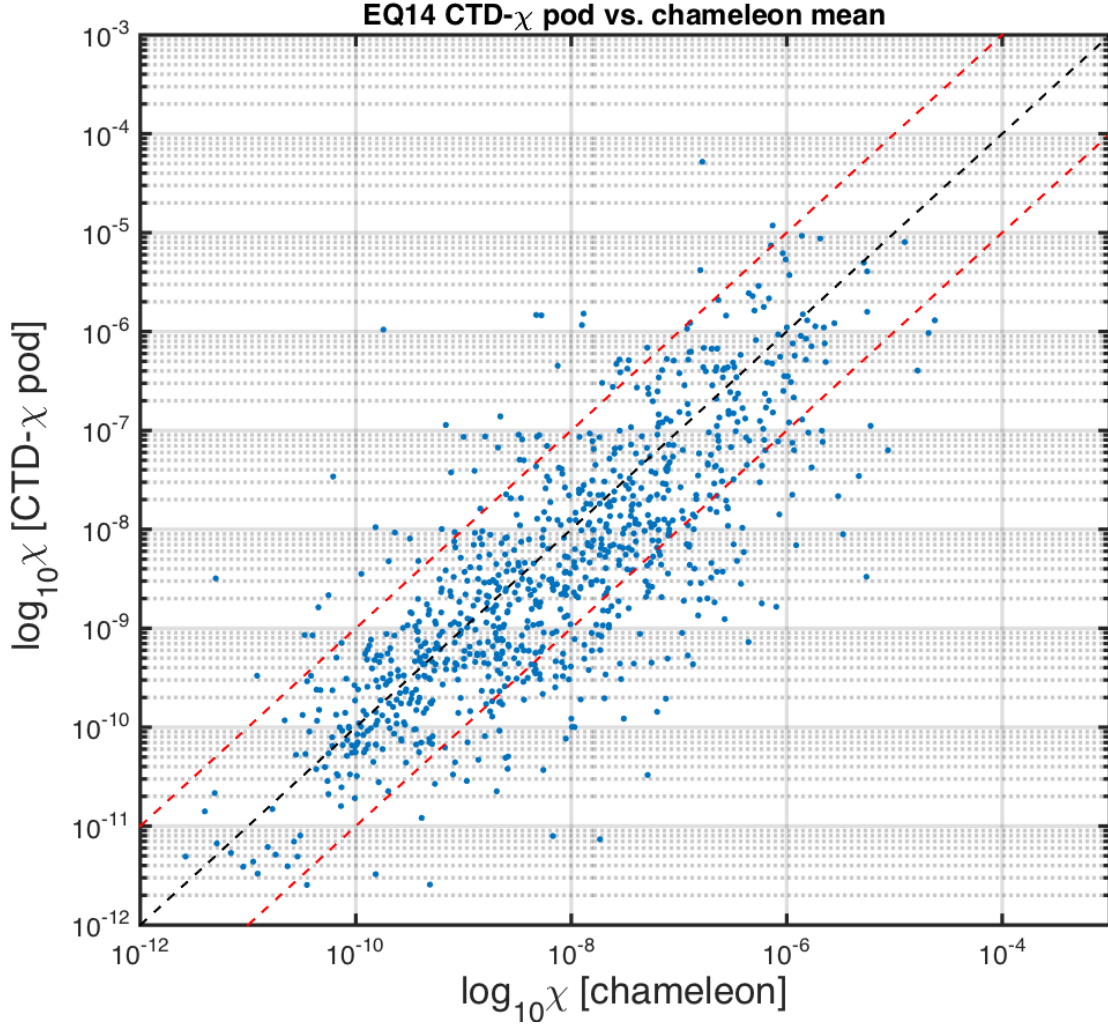


FIG. 9. Scatter plot of χ from CTD- χ pod profiles versus the mean of bracketing chameleon profiles. Black
dashed line shows 1:1, red are ± 10 X. **replace with histogram of ratios, or combine into one figure?**

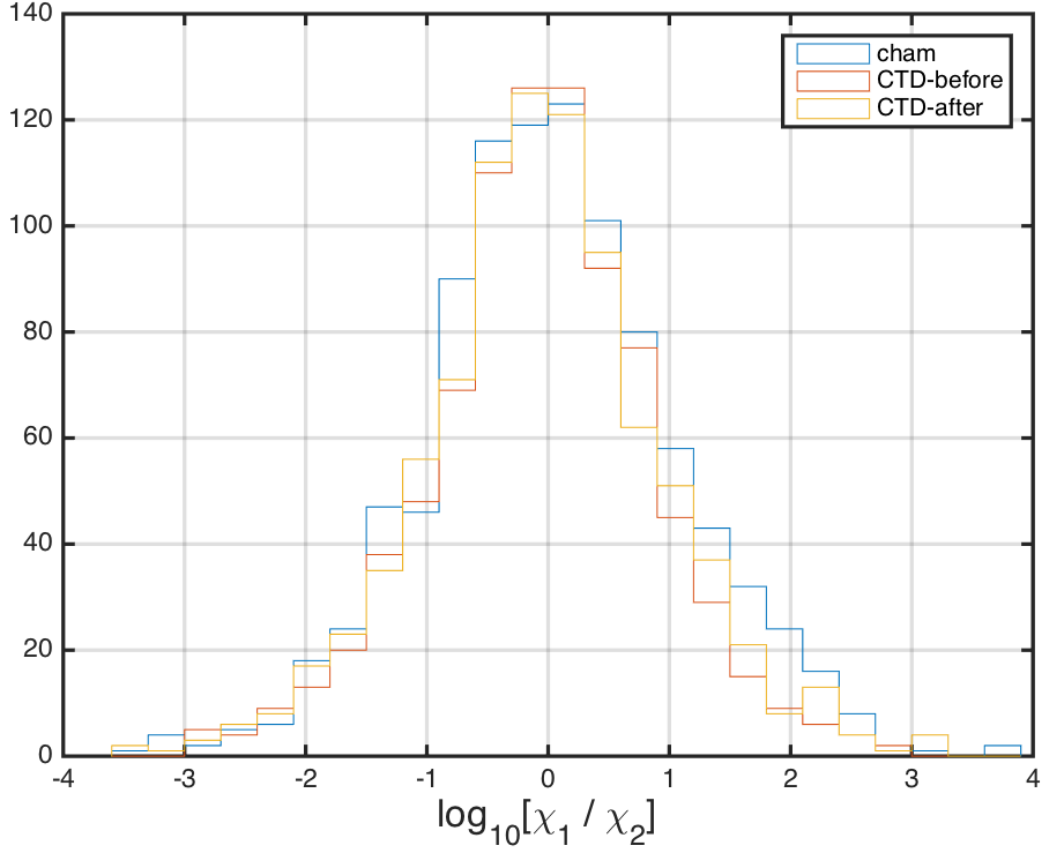


FIG. 10. Histogram of \log_{10} of the ratio of χ for nearby casts. One line is for CTD- χ pod profiles versus the bracketing chameleon profiles. Another line is for the before vs. after chameleon profiles. *Note bias is small/zero, and the variability (spread) between CTD/cham is similar to the natural variability between cham profiles.*

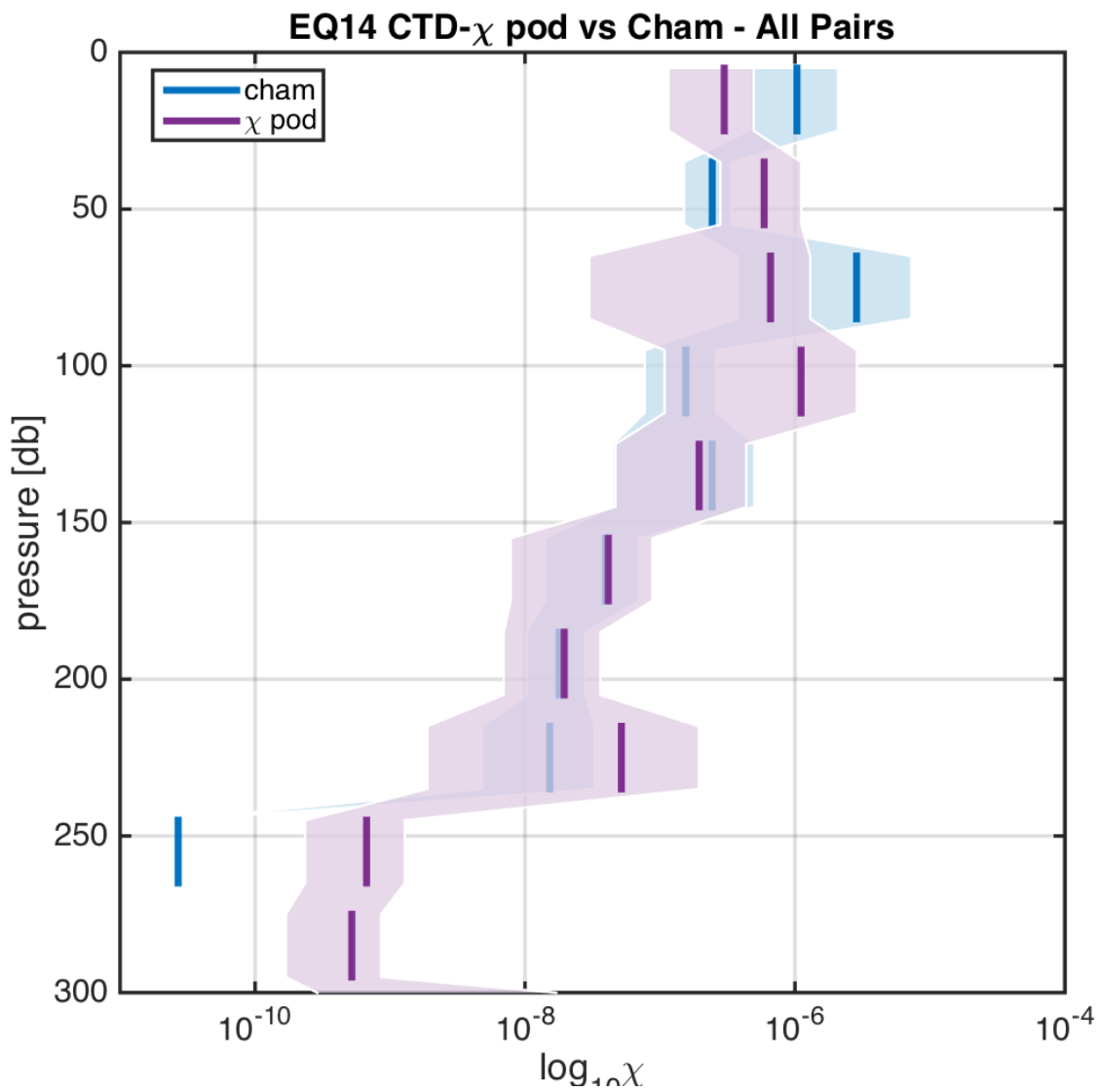


FIG. 11. Time mean of χ for all CTD- χ pod - chameleon cast pairs, with 95% bootstrap confidence intervals.

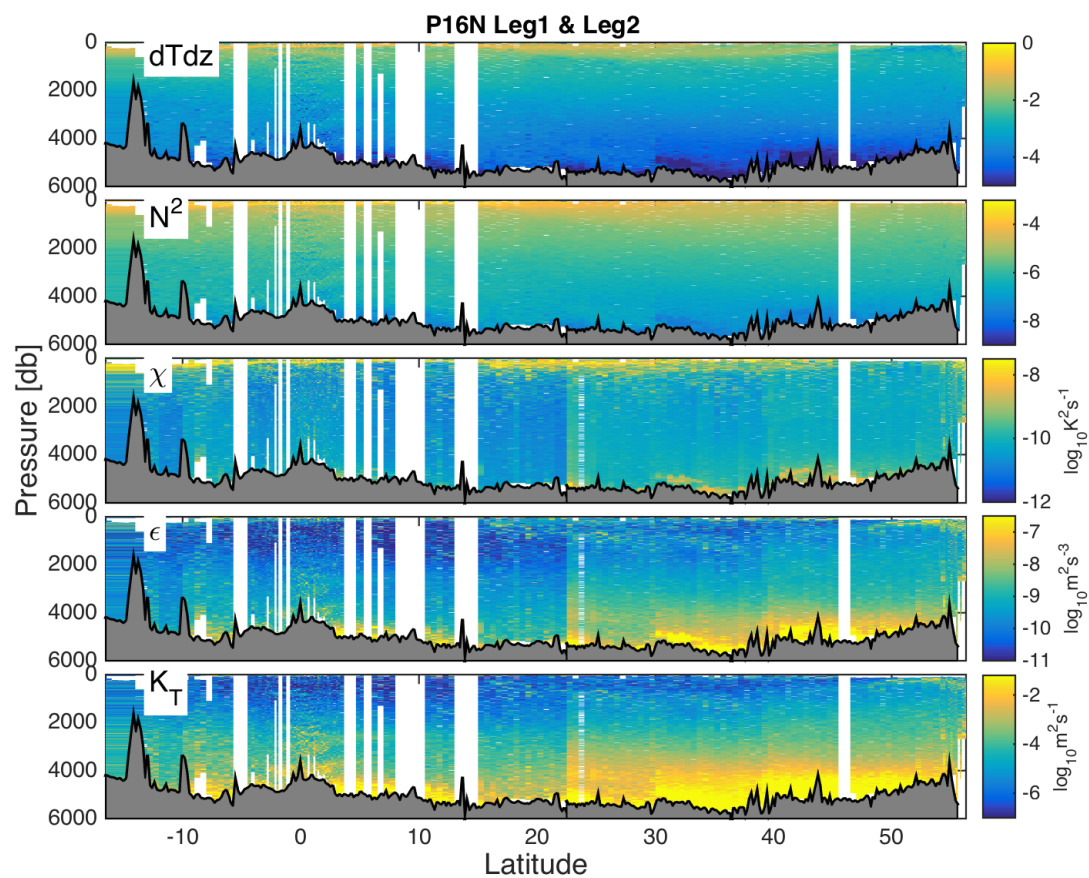


FIG. 12. Example chipod data from P16N. *need to clean up*

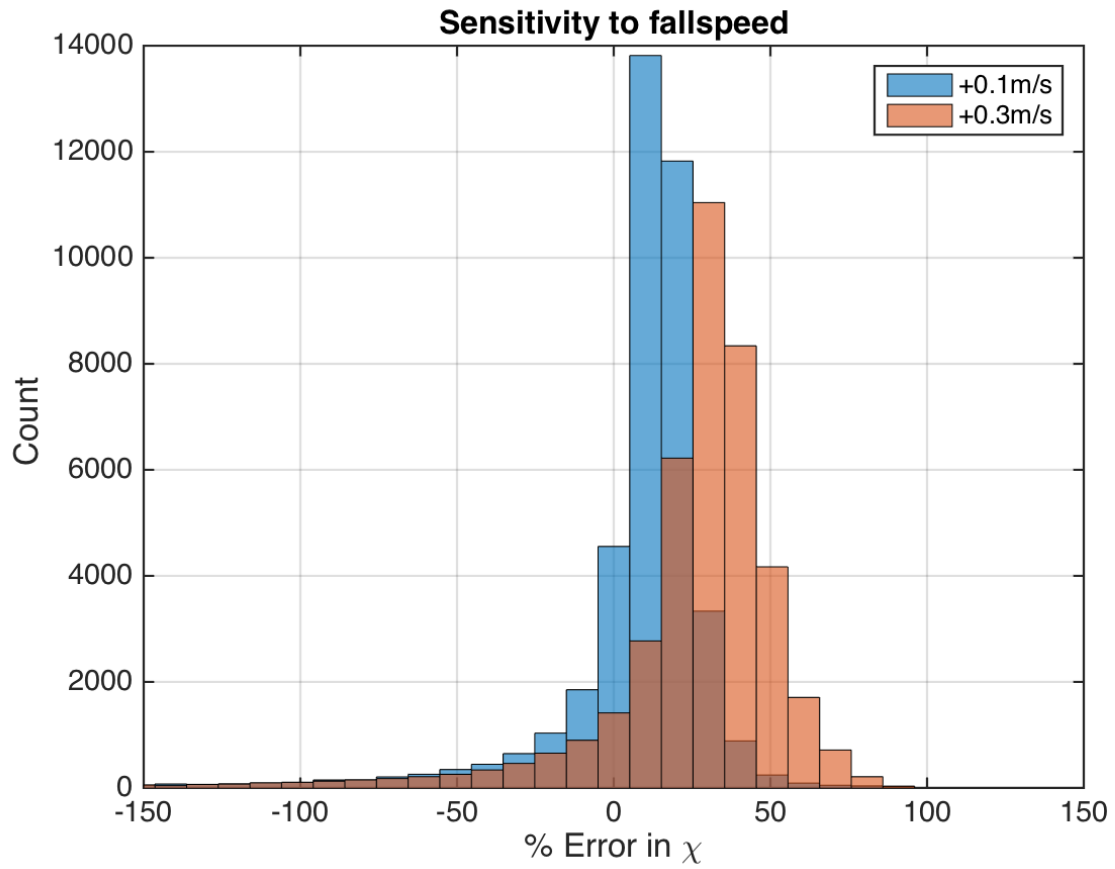


FIG. 13. Histogram of % error for χ computed with constant \pm fspd added.